Journal of Applied Mechanics and Technical Physics, Vol. 45, No. 6, pp. 822–827, 2004

INVESTIGATION OF NONUNIFORMITY OF THE VELOCITY DISTRIBUTION IN THE SHEAR LAYER OF AN UNDEREXPANDED JET BY ELECTRIC DISCHARGE TRACING OF THE FLOW

V. I. Zapryagaev, A. P. Petrov, and A. V. Solotchin

UDC 533.6.011

Streamwise and radial components of velocity in the shear layer of an underexpanded jet are measured by the method of spark tracing. The nonuniform distribution of gas-dynamic parameters of the flow in this region is caused by streamwise Görtler-type vortex structures.

Key words: *supersonic underexpanded jet, shear layer, Taylor–Görtler vortices, spark tracing of the flow.*

Determination of parameters of a supersonic flow by measuring the static pressure and stagnation pressure behind the normal shock by means of pneumatic probes is not always correct because of the nonuniform distribution of the measured quantities. Such a situation is typical in studying the shear layer of an underexpanded jet. Using a Pitot tube, it is possible to measure the total pressure distribution in this flow region [1, 2], whereas the measurement accuracy for static pressure is insufficient for obtaining reliable results in velocity-field studies because of the curvature of streamlines in the compressed layer [3]. Under these conditions, it is reasonable to prefer direct measurements of flow velocity by the method of electric discharge tracing of the flow [4] with the use of a channel of an ionized gas formed owing to the high-voltage electric discharge at the flow segment between the electrodes. Because of the high repetition frequency of the discharge, it is possible to visualize the wake of the ionized track at different times and at different distances from the primary spark. Direct measurements of flow velocity can be performed in a short time by electric discharge tracing, which was demonstrated by measuring the velocity of a one-dimensional flow [5, 6].

Instantaneous fields of velocity components in the shear layer of a supersonic axisymmetric underexpanded jet are constructed in the present work on the basis of results of electric discharge tracing of the flow.

The experimental studies of velocity distributions were performed on a vertical jet facility in the shear layer of the initial part of the underexpanded jet with a Mach number at the nozzle exit $\mathrm{M}_a = 1$ and a nozzle-pressure ratio $n = p_a/p_h = 2.65$ (p_a is the pressure in the nozzle-exit cross section and p_h is the ambient pressure). The nozzle-exit radius was 10 mm. The Reynolds number based on flow parameters at the nozzle exit was $\mathrm{Re}_d = 1.71 \cdot 10^6$, where $d = 20$ mm. The nozzle was manufactured from a dielectric material (caprolactam). The electrodes of the spark generator were located in the flow so that the segment of the examined jet was located between them. Simultaneously with formation of electric discharges, the sparks were photographed by two cameras. The configuration of the jet centerline and optical axes of the cameras was a rectangular parallelepiped whose lower base coincided with the plane of the nozzle-exit section and the rib NK coincided with the jet centerline (Fig. 1). The camera F was located in the opposite corner of the upper base. Hence, the diagonal MK of the parallelepiped coincided with the optical axis of the upper camera. The angle between the diagonal plane $MNKL$ and the side face $NN'K'K$ was $\alpha = 32°$, and the angle $K'N'K$ was $\beta = 27°$. In analyzing the two-dimensional flow pattern and calculating velocity-vector components, we took into account the geometric features of the relative positioning of the object under study and optical instruments.

Institute of Theoretical and Applied Mechanics, Siberian Division, Russian Academy of Sciences, Novosibirsk 630090; zapr@itam.nsc.ru. Translated from Prikladnaya Mekhanika i Tekhnicheskaya Fizika, Vol. 45, No. 6, pp. 58–64, November–December, 2004. Original article submitted October 10, 2003; revision submitted January 12, 2004.

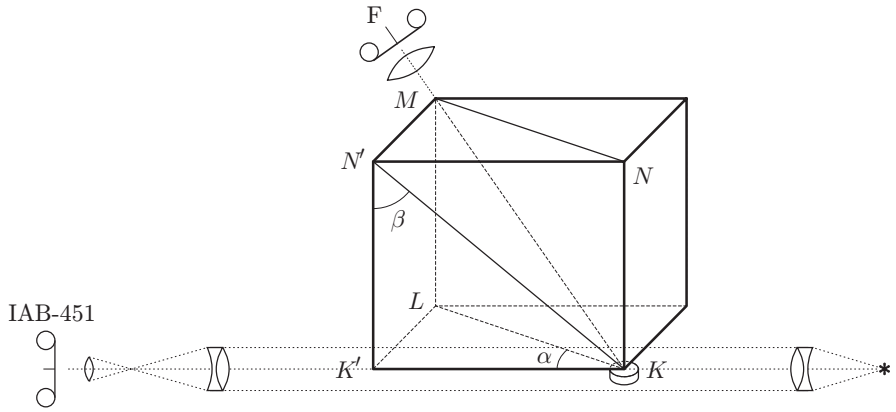

Fig. 1. Position of the object under study and optical instrumentation.

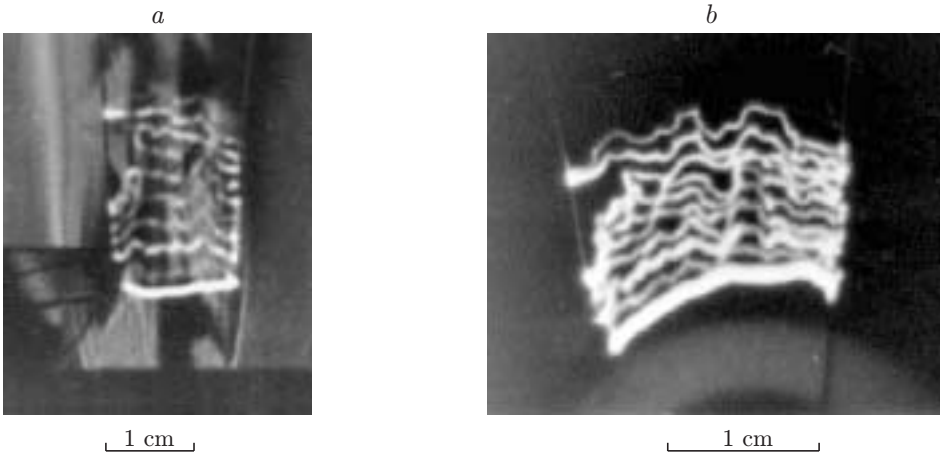

Fig. 2. Photographs of electric discharge sparks, obtained through the IAB-451 optical device (a) and by the upper camera (b).

The electrodes were two tense wires 0.3 mm thick insulated from each other. One wire was grounded, and the other was connected to a high-voltage pulse generator and was introduced into the supersonic jet flow on a moving sting made of a dielectric material. This induced oblique shock waves, but there exists no other method of introducing electrodes into the flow without formation of shock waves. The minimum distance between the electrodes corresponded to the value at which a spark breakdown was possible. The time interval of the repeated spark pulse was 6 μsec, and the discharge-pulse duration was approximately 0.3 μsec. The ionized channel formed after the first electric discharge was entrained downstream with the flow velocity. The first spark discharge passed over the shortest way between the electrodes; its position was constant and located at a distance of 9.3 mm from the nozzle. The second and later discharges followed the ionized channel, and their position in the flow depended on the time interval between the discharges and on the local flow velocity.

Figure 2 shows the photographs obtained in the experiment. The object under study was photographed simultaneously from two positions: through the IAB-451 optical device (Fig. 2a) and from the upper position at a certain angle to the optical axis of the IAB-451 device (Fig. 2b). In the first case, we observe overlapping of the Schlieren picture of the jet with the system consisting of ten spark discharges obtained from the generator of high-voltage pulses with a frequency of approximately 167 kHz. The combination of the spark tracing method with shadowgraphy allowed visualization of the wave structure of the flow and position of discharges in the flow, as well as determination of the streamwise component of velocity for each position of the spark. The second photograph shows the same system of sparks observed from above.

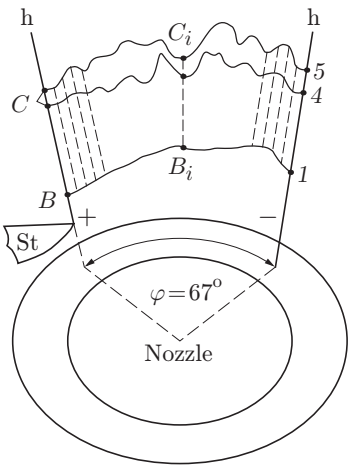

Fig. 3. Scheme of three spark discharges registered by the upper camera: 1) first spark; 4) fourth spark; 5) fifth spark; the electrode sting is indicated by St; the electrodes are denoted by h; the electrodes connected to the high-voltage pulse generator and grounded are indicated by plus and minus, respectively.

The ionized track entrained by the flow changed its initial shape because of the nonuniformity of velocity distribution in the shear layer of the jet. Subsequent electric discharges passing over this path were registered on the photographic film in the form of aperiodic wave lines in different cross sections of the shear layer. The amplitude and frequency of the waves are determined by the Taylor–Görtler vortices, since a secondary flow arises in local segments of the jet in the flow with such vortices; interaction of this secondary flow with the main stream leads to formation of streamwise and radial (transverse) velocity components.

The photographs of spark discharges were scanned and fed into a computer for further processing. To determine the distance between the first and subsequent sparks, the images of spark tracks were supplemented by lines spaced by 1 degree so that their total angle corresponded to the azimuthal angle of the sweep. A special program for graphical representation of intensity distribution in the cross section of the spark discharge on the photograph was used [7]. This allowed more exact determination of the coordinates where the lines intersected the middle points of the spark tracks. The data obtained for the corresponding spark discharges were tabulated and used further to determine velocity components.

The error of velocity measurement by the method of spark tracing of the flow is within 5% according to [6]. In addition, the accuracy of flow measurements by this method is affected by a number of factors. In the present study, these are primarily shock waves generated by the sting and electrodes. In the photographs (see Fig. 2), the spark discharges of the 6th, 7th, and 8th sparks on one electrode have a common point, which is apparently associated with the influence of the shock wave from the sting. Therefore, tracks located upstream of disturbances caused by shock waves were used to determine velocity in the shear layer.

Figure 3 shows the first, fourth, and fifth sparks from Fig. 2b. The track of the first spark discharge was used as the basic spark for measurement of distances between the tracks. Figure 4 shows part of the profile of the underexpanded jet and the electrode h–h located in the shear layer. The points on the electrode show the schematic tracks of ten spark discharges following with an identical time interval $\Delta\tau$. During the exposure time, the ionized channel was shifted along the electrode from the point A to the point C and was registered by the camera F as the projection BC to the plane EE aligned with the film. In the right triangle ACD built on the basis of the first and subsequent sparks, the legs AD and DC are the radial and axial components of the calculated characteristics of the flow of the corresponding spark track. The angle of inclination of the hypotenuses γ_i in the triangles $(ACD)_i$ is γ only if the distance $(BC)_i$ between the first and subsequent sparks equals the distance BC on the electrodes, i.e., as is the case at the edges of the sweep (see Fig. 3). Here, i are the numbers of the calculated points on the sweep. In the remaining cases, the slope of the hypotenuses can be greater or smaller than γ. If we have the distance $(BC)_i < BC$, the angle at the triangle apex $(ACD)_i$ is smaller than γ, i.e., $\gamma' = \gamma - \Delta\gamma$; if $(BC)_i > (BC)$, then

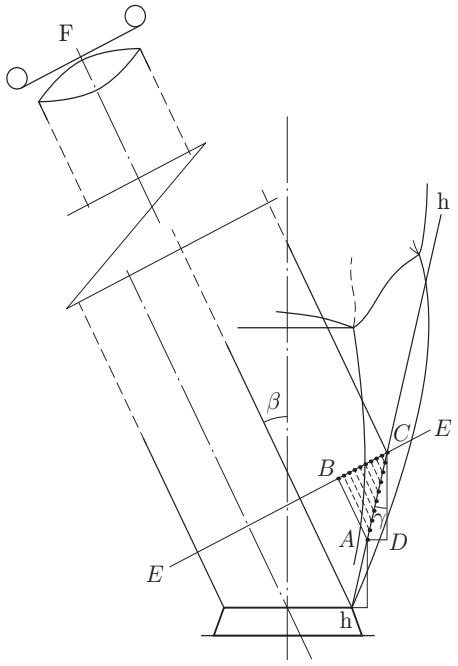

Fig. 4. Part of the jet profile and electrode located in the shear layer (the comments are given in the text).

we have $\gamma'' = \gamma + \Delta\gamma$. Here, we obtain

$$\gamma' = \gamma - \Delta\gamma = \arctan\Big(\tan\gamma + \frac{(-bc)_i \sin(\beta+\gamma)}{BC\cos\gamma}\Big); \tag{1}$$

$$\gamma'' = \gamma + \Delta\gamma = \arctan\Big(\tan\gamma + \frac{(bc)_i \sin(\beta+\gamma)}{BC\cos\gamma}\Big), \tag{2}$$

where $(\pm bc)_i = (BC)_i - BC$.

The Mach numbers of the axial and radial components are

$$(\mathrm{M}_x)_i = (A_x)_i/(\tau_\Sigma c), \qquad (\mathrm{M}_r)_i = (A_r)_i/(\tau_\Sigma c). \tag{3}$$

The total time of motion of the ionized track from the first spark discharge to the calculated point is

$$\tau_\Sigma = [\tau(m-1) + \Delta\tau m]\cdot 10^{-6} c. \tag{4}$$

Here τ is the time interval of spark formation, m is the spark number, $\Delta\tau$ is the spark-discharge duration, and c is the local velocity of sound, $(A_x)_i$ and $(A_r)_i$ are the streamwise and radial components of displacement of spark discharges. Within the range of variation of the azimuthal angle $\varphi = 0$–$67°$, we used the geometric representation of the examined object in Fig. 4 to obtain the following expressions for the quantities $(A_x)_i$ and $(A_r)_i$:

$$(A_x)_i = (DC)_i = \frac{(BC)_i \cos(\gamma \pm \Delta\gamma)}{k\cos\alpha\sin[\beta + (\gamma \pm \Delta\gamma)]}; \tag{5}$$

$$(A_r)_i = (AD)_i = \frac{(BC)_i \sin(\gamma \pm \Delta\gamma)}{k\cos\alpha\sin[\beta + (\gamma \pm \Delta\gamma)]} \tag{6}$$

(k is the scale of the examined object in the photograph).

The distributions of the streamwise and radial components of the Mach number on the fourth and fifth spark tracks in Fig. 5 reveal significant nonuniformity of flow parameters not only in the streamwise but also in the radial direction. It follows from a comparison of the dependences in Fig. 5 that the axial and radial components of the Mach number are in antiphase.

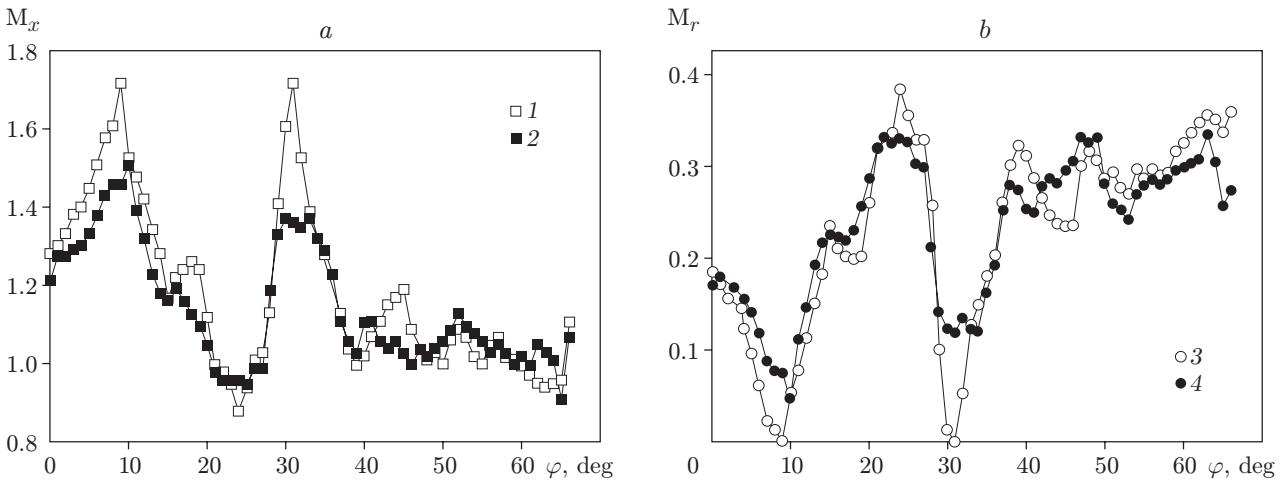

Fig. 5. Nonuniformity of the streamwise (a) and radial (b) components of the Mach number versus the azimuthal angle φ: points 1 and 3 refer to the fourth spark; points 2 and 4 refer to the fifth spark; $(x/R_a)_4 = 1.7$; $(x/R_a)_5 = 1.96$.

Based on the previous measurements and theoretical calculations (see [1, 2, 8, 9]) of the dynamics of total pressure variations over the azimuth of the shear layer of a supersonic underexpanded jet, a hypothesis was put forward that the nonuniformity of gas-dynamic parameters in the near-wall part of the flow is caused by streamwise vortex structures, such as the Taylor–Görtler vortices. These vortices are quasi-steady disturbances formed in flows with curved streamlines [10]. It is assumed that the axes of the streamwise vortices are parallel to the streamlines in the middle of the shear layer. The wavelength of these disturbances corresponds to two counterrotating streamwise vortices. Hence, the vortex structure of a supersonic jet is a closed circular structure composed of counterrotating vortices. For this reason, the flow structure in the shear layer and in the adjacent boundary layer is characterized by periodic suction of the low-pressure gas from the ambient medium or by entrainment of the high-velocity gas from the compressed layer. Aperiodic nonuniformity over the azimuthal coordinate is observed not only for the total pressure but also for flow velocity. The secondary flow generated by streamwise vortices has a certain but variable momentum. The momentum of the secondary flow depends on intensity of the corresponding pair of vortices, i.e., on intensity of individual modes of the spectrum of nonuniformity of velocity and total pressure distributions [11].

It seems important to consider the spatial evolution of disturbances in the flow region considered. If we assume that the middle of the span of nonuniformity of the radial component coincides with the middle of the shear layer, the maximum deviations of nonuniformity from the jet centerline corresponding to azimuthal angles $\varphi = 23$, 48, and 63° reach the outer boundary of the shear layer of a supersonic jet where the Mach number equals unity. The streamwise and radial components of the Mach number for these azimuthal angles (see Fig. 5) are $M_x = 0.96$, 1.00, and 0.92; $M_r = 0.34$, 0.33, and 0.34, respectively. The calculation of velocity on the basis of its measured components shows that the flow Mach number in the jet is approximately equal to unity, namely, $M = 1.02$, 1.05, and 0.98. These data are in satisfactory agreement with the results of studying gas-dynamic characteristics of the jet [3, 12]. Returning to streamwise vortex structures, we can state that rotation of vortices at these azimuthal angles facilitates entrainment of the high-velocity flow to the jet periphery, which allows the radial components of velocity to reach the greatest value. The velocity of the streamwise components is close to the velocity of sound.

The distribution of flow characteristics at azimuthal angles $\varphi = 10$, 31, and 52° is absolutely different. The radial components of nonuniformity of the spark track are directed toward the inner boundary of the shear layer, and the streamwise components reach a maximum. The flow Mach number of streamwise and radial components are $M_x = 1.55$, 1.37, and 1.13; $M_r = 0.04$, 0.12, and 0.24. The flow Mach number in the jet at these azimuthal angles is either equal to the Mach number of the streamwise component or insignificantly differs from it, namely, $M = 1.55$, 1.38, and 1.16.

In the case considered, the pairs of streamwise vortices have such a direction of revolution at which the low-pressure flow is discharged from outside toward the inner boundary of the shear layer adjacent to the compressed

layer where the flow velocity is supersonic. In this case, the radial component of velocity of the low-pressure flow is decelerated, and the resulting velocity corresponds almost completely to the streamwise component. Hence, depending on the direction of revolution of streamwise vortices, there occurs a periodic redistribution of mass and momentum of secondary flows and also kinetic energy between velocity components. The gas flow of the radial component of velocity has a higher kinetic energy in the case of entrainment of the high-velocity flow from the shear layer than in the case of discharge of the low-pressure gas. The gas flow in the streamwise direction, vice versa, acquires a higher kinetic energy in the case of discharge of the low-pressure flow to the shear layer.

Thus, direct measurements of the distribution of two components of flow velocity in the shear layer of a supersonic underexpanded jet were performed with the help of spark tracing of the flow. The special features of the jet region considered are caused by the loss of hydrodynamic stability; as a result of the latter, disturbances in the form of streamwise vortex structures are formed in the shear layer. The streamwise vortices facilitate flow reconstruction in the jet, leading to a nonuniform distribution of gas-dynamic characteristics over the azimuthal coordinate.

This work was supported by the Russian Foundation for Basic Research (Grant No. 02-01-00515).

REFERENCES

1. V. I. Zapryagaev and A. V. Solotchin, "Spatial flow structure at the initial part of a supersonic underexpanded jet," Preprint No. 23-88, Inst. Theor. Appl. Mech., Sib. Div., Acad. of Sci. of the USSR, Novosibirsk (1988).
2. V. I. Zapryagaev and A. V. Solotchin, "Three-dimensional structure of flow in a supersonic underexpanded jet," *J. Appl. Mech. Tech. Phys.*, **32**, No. 4, 503–507 (1991).
3. V. I. Zapryagaev, A. V. Solotchin, and N. P. Kiselev, "Structure of a supersonic jet with varied geometry of the nozzle entrance," *J. Appl. Mech. Tech. Phys.*, **43**, No. 4, 538–543 (2002).
4. P. G. Zykov, A. M. Filatov, and P. E. Suetin, "Gas-flow velocity measurement by the method of multiple spark breakdown," *Prib. Tekh. Éksp.*, No. 2, 195–197 (1976).
5. V. N. Rychkov and M. E. Topchiyan, "Direct measurement of hypersonic flow velocity by the method of electric discharge tracing," *Teplofiz. Aéromekh.*, **6**, No. 2, 173–180 (1999).
6. Yu. V. Afonin, A. P. Petrov, and D. G. Nalivaichenko, "Application of a multichannel high-voltage pulse generator for visualization and measurement of gas-flow velocity," *Teplofiz. Aéromekh.*, **9**, No. 1, 143–149 (2002).
7. V. M. Boiko, V. I. Zapryagaev, V. I. Kornilov, et al., "Further development of the spark tracing technique for flow visualization," in: *Proc. of the Int. Conf. on the Methods of Aerophysical Research* (Novosibirsk, 1–7 July, 2002), Part. 1, Publ. House "Nonparel," Novosibirsk (2002), pp. 40–44.
8. N. A. Zheltukhin, V. I. Zapryagaev, A. V. Solotchin, and N. M. Terekhova, "Spectral composition and structure of stationary Taylor–Görtler vortices in a supersonic jet," *Dokl. Akad. Nauk SSSR*, **325**, No. 6, 1133–1137 (1992).
9. N. A. Zheltukhin and N. M. Terekhova, "Taylor–Görtler instability in a supersonic jet," *J. Appl. Mech. Tech. Phys.*, **34**, No. 5, 640–646 (1993).
10. G. Schlichting, *Boundary Layer Theory*, McGraw-Hill, New York (1968).
11. V. I. Zapryagaev, A. V. Solotchin, and N. P. Kiselev, "Streamwise vortex structures in a supersonic jet shear layer," in: *Proc. West East High Speed Flow Fields, Aerospace Applications from High Subsonic to Hypersonic Regime*, CIMNE, Barcelona (2003), pp. 299–305.
12. V. N. Glaznev and Sh. Suleimanov, *Gas-Dynamic Parameters of Weakly Underexpanded Free Jets* [in Russian], Nauka, Novosibirsk (1980).